Gene 977 (2026) 149840

Contents lists available at ScienceDirect

Gene

journal homepage: www.elsevier.com/locate/gene

Research paper

Expression analysis of androglobin and its influence on the transcriptome in cancer

Carina Osterhof [a,b], Michel Seiwert [a], Stefan Mündnich [a], Teng Wei Koay [b], Elena Porto [a], Glen Kristiansen [c], David Hoogewijs [b,**], Thomas Hankeln [a,*]

[a] Institute of Organismic and Molecular Evolution, Molecular Genetics and Genome Analysis, Johannes Gutenberg University, Mainz, Germany
[b] Department of Endocrinology, Metabolism and Cardiovascular System, University of Fribourg, Fribourg, Switzerland
[c] Institute of Pathology, Center for Integrated Oncology, University Hospital Bonn, University of Bonn, Bonn, Germany

ARTICLE INFO

Edited by: Marianna Kruithof-deJulio

ABSTRACT

Androglobin (ADGB) is a phylogenetically ancient multi-domain protein with an embedded globin domain, which binds heme and may therefore interact with gaseous molecules. Other globins like neuroglobin, cytoglobin and myoglobin have shown tumor-suppressor or oncogenic roles in a tissue-dependent way, and also ADGB has been suggested as being oncogenic in prostate and brain cancer models. However, *ADGB* expression in human tumor entities *in vivo* has not been investigated systematically so far. Here we mined transcriptome data from various cancer types and reveal that *ADGB* is typically downregulated in cancer cell lines, as well as in tumors from lung and testis, which express *ADGB* endogenously in healthy states. We show via bioinformatics analyses that in cell lines only a few *ADGB* exons are transcribed, or the gene locus was amplified, which greatly limits suitability of such cell lines as model systems for research into ADGB. Consistent with correlation analysis, we further demonstrate that RFX3 regulates *ADGB* promoter-driven luciferase activity as well as endogenous *ADGB* expression levels. Since recent literature postulated oncogenic effects of ADGB, we established stable *ADGB* overexpression (ADGB+) in A549 lung cancer cells. Our transcriptomic analysis of ADGB + cells indicate increased cell motility and restructuring of the extracellular matrix – both hallmarks of elevated malignancy. ADGB thus may display oncogenic potential *in vitro*. However, since human cancer entities show little to no *ADGB* transcription, a role for ADGB in tumorigenesis *in vivo* appears rather limited.

1. Introduction

Globins are an evolutionary ancient family of proteins, which form a hydrophobic pocket (the so-called globin-fold) that allows the binding of a heme prosthetic group. The members of this protein family perform a wide variety of functions (Burmester and Hankeln, 2014; Keppner et al., 2020), but vertebrate globins, such as hemoglobin or myoglobin, are especially known for their vital role in oxygen supply and transport (Wittenberg and Wittenberg, 2003). In addition, both respiratory proteins have the ability to either produce or scavenge reactive oxygen and nitrogen species depending on the concentration of oxygen in their surroundings (Flögel et al., 2001; Hendgen-Cotta et al., 2008). By this property, globins have been reported to promote or inhibit tumor growth. Several members of the globin family are in fact deregulated in human cancer entities and may even have prognostic value. The expression of Myoglobin (MB), for example, is upregulated in colon and breast cancer (Flonta et al., 2009; Gorr et al., 2011; Kristiansen et al., 2010). Depending on the tissue of origin, MB expression is either associated with a favorable outcome like in breast cancer (Kristiansen et al., 2010), and head and neck squamous cell carcinoma (Meller et al., 2016) or with a more aggressive tumor phenotype e.g. in glioma (Elsherbiny et al., 2021). Cytoglobin (CYGB), a vertebrate globin type mostly

Abbreviations: ADGB, Androglobin; BH, Benjamini-Hochberg; BSA, bovine serum albumin; ChIP, chromatin immunoprecipitation; CYGB, Cytoglobin; ECM, extracellular matrix; GO, gene ontology; GTEx, Genotype-Tissue Expression; HPA, Human Protein Atlas; lincRNA, long intergenic non-coding RNA; LUSC, lung small cell carcinoma; MB, Myoglobin; NGB, Neuroglobin; PBS, phosphate-buffered saline; Pen/Strep, Penicillin/Streptomycin; PFA, paraformaldehyd; qRT-PCR, quantitative reverse-transcription PCR; RNA-Seq, RNA-Sequencing; TCGA, The Cancer Genome Atlas Program; TPM, transcripts per million.

* Corresponding author.
** Corresponding author.
E-mail addresses: david.hoogewijs@unifr.ch (D. Hoogewijs), hankeln@uni-mainz.de (T. Hankeln).

https://doi.org/10.1016/j.gene.2025.149840
Received 22 May 2025; Accepted 14 October 2025
Available online 24 October 2025

expressed in connective tissue cells of many organs, is often downregulated in tumors via hypermethylation of its promoter, e.g. in esophageal cancer, non-small cell lung cancer and head and neck squamous carcinoma (Oleksiewicz et al., 2011). Knockout of Cygb in two mouse models showed a higher susceptibility for neoplasia in liver, lung, and colon (Thuy et al., 2011; Yassin et al., 2018). In line with this, decreased CYGB expression was correlated with more frequent tumor recurrence and poor prognosis in glioma as well as in pancreatic ductal adenocarcinoma patients (Kono et al., 2021; Xu et al., 2013). CYGB also modulates cancer therapy sensitivity in a melanoma model (De Backer et al., 2022). For neuroglobin (NGB), a globin variant mostly expressed in neurons of the nervous system (Burmester et al., 2000), a dualistic function in cancer progression has been proposed. While it may act as a tumor suppressor in hepatocellular carcinoma and pancreatic cancer (Wu et al., 2023; Zhang et al., 2013), its upregulation is associated with poorer prognosis in glioma patients (Zhang et al., 2017). In glioma and breast cancer cell models, endogenous NGB showed an anti-apoptotic function and promoted proliferation (Fiocchetti et al., 2018; Zhang et al., 2018a), but the strength of endogenous expression is debatable for the MCF-7 model (Fabrizius et al., 2016). Despite many still open questions, these results suggest that globins may represent interesting candidates for cancer research.

An additional, but structurally divergent member of the vertebrate globin family is androglobin (ADGB) (Hoogewijs et al., 2012). ADGB's globin domain is embedded in a larger protein which carries high resemblance with a calpain protease. In addition, the ADGB globin domain is permutated and interrupted by a putative calmodulin binding site. In analogy to other family members, the gene/protein name was designed to hint at its predominant expression site, since ADGB was initially reported to be mainly expressed in later stages of spermatogenesis in mammalian testes (Hoogewijs et al., 2012). Functional studies performed in an *Adgb* knockout mouse model revealed a vital role for Adgb during spermatogenesis (Keppner et al., 2022). Subsequently, *ADGB* expression was recognized to be a marker of multi-ciliated cells from lung, brain and also the female reproductive tract, where its expression is probably regulated by FOXJ1, the master transcription factor of ciliogenesis (Koay et al., 2021). This strong association with ciliated cells suggests a direct function in ciliogenesis, while ADGB's exact mode of action is still unclear. ADGB has also been studied in the context of cancer before. An *in vitro* cell culture study suggested that *ADGB* could act as an oncogene in glioma formation (Huang et al., 2014). Another study proposed that epigenetic silencing of *ADGB* via the lncRNA STXBP5-AS1 reduces cell stemness in pancreatic cancer (Chen et al., 2020). Besides this, however, the expression pattern and possible functional role of ADGB in a tumor context remains elusive. We therefore characterized the expression levels of *ADGB* in different human cancer entities and during cancer progression with the aim to analyze whether ADGB could influence tumorigenesis *in vivo*.

2. Results

2.1. ADGB is downregulated in tumorous tissues and cell lines

To examine *ADGB* mRNA expression during tumorigenesis, we mined public RNA-Seq data from individual experiments as well as from several research consortia that analyzed large numbers of samples from cancerous tissues and commonly used cell lines. For the individual datasets, we quality-processed and mapped deposited raw read data, and quantified *ADGB* expression to ensure comparability. For data from large consortia, we used analysed and harmonized read counts and TPM values, whenever available.

Since lung is an endogenous *ADGB* expression site and also frequently gives rise to cancer, we firstly reanalyzed publicly available RNA-Seq datasets on lung cancer progression in humans. We found a significantly lower amount of *ADGB* mRNA expression in fully developed squamous cell carcinoma (Ooi et al., 2014) in comparison to normal basal cells (Fig. 1a). There was also a tendency towards lower levels of *ADGB* transcripts in premalignant cell lesions, however, this was not statistically significant. The second study (Morton et al., 2014) showed a similar result, with significantly lower *ADGB* levels in invasive lung carcinomas. *ADGB* mRNA was downregulated in every patient analyzed (n = 6, Fig. 1b).

Next, we investigated the extensive TCGA datasets (https://portal.gdc.cancer.gov/; Fig. 2a) with a focus on tissues with endogenous *ADGB* expression (Koay et al., 2021). The downregulation of *ADGB* mRNA expression could again be verified in tumor entities from testis and lung. We validated these findings via qPCR in paired normal and tumor tissue samples from human testis and lung of an independent cohort (Figs. 1c, d). Absolute expression of *ADGB* mRNA was lower in every tumor sample compared to its healthy counterpart. The TCGA data also showed a (non-significant) tendency towards higher levels of *ADGB* mRNA in two types of uterine cancer (Fig. 2a). However, there was no difference in *ADGB* mRNA levels between glioblastoma multiforme, brain lower grade glioma, pancreatic adenocarcinomas, and their respective healthy tissues (Fig. 2b).

In summary, *ADGB* mRNA expression decreases during cancer progression in testis and lung tissue, but the initial amount of *ADGB* in healthy tissue varies greatly. This is probably due to *ADGBs* strict cell type-specific expression pattern and different proportions of ciliated cells in the analyzed samples (Koay et al., 2021).

In light of other studies which suggested an oncogenic function of ADGB *in vitro* (Chen et al., 2020; Huang et al., 2014), we screened a variety of public databases with transcriptome information on cell lines. Of the 1207 cell lines sequenced by the Cancer Cell Line Encyclopedia (Barretina et al., 2012; Ghandi et al., 2019) and Human Protein Atlas consortium, only 2 showed *ADGB* mRNA expression, albeit at low amounts: lung cancer NCIH2106 (TPM 4.7) and Hodgkin lymphoma HDLM2 (TPM 5.3) (Fig. 3). Intriguingly, genomic resequencing data and subsequent gene copy number analysis derived from the DepMap portal suggested that elevated *ADGB* expression in NCIH2106 is not due to modulation of *ADGB* regulation, but probably a consequence of an increased number of gene copies in this cell line, making it unsuitable for knockout studies. For the HDLM-2 cell line, we re-analyzed transcriptome data of HDLM-2 from two independent studies. *ADGB* was indeed expressed in both with TPM values of 7.63, 6.48, 9.91 (PRJNA668062) and 1.85 (PRJEB30312), respectively. Visual inspection of the alignments, however, revealed that the cDNA reads covered only the last 4 exons of the *ADGB* gene locus (S1 Fig). This indicates that the HDLM-2 cell line may exclusively express a truncated version of the gene which neither encompasses the calpain, nor the globin and calmodulin-binding domains of ADGB. Of note, we found no RNA-Seq evidence for endogenous *ADGB* transcription in glioblastoma cell lines U87 and U251 (Fig. 3, "Brain cancer"). This is in some contrast to a study which reported the effects of *ADGB* knockdown in those cell models and measured *ADGB* transcription via qRT-PCR (Huang et al., 2014).

2.2. Correlation analysis implies complex ADGB regulation

Recently, a possible mechanism for the observed downregulation of *ADGB* mRNA was proposed. A study suggested that the expression of LncRNA *STXBP5-AS1* and subsequent recruitment of transcription factor EZH2 lead to heavy methylation and thus silencing of the *ADGB* promoter (Chen et al., 2020). In consequence, tissues with high levels of *STXBP5-AS1* should show lower levels of *ADGB* mRNA. It seems, however, that the downregulation of *ADGB* in tumorous tissues might follow a different mechanism, since we did not find evidence for the expected inverse correlation of *STXBP5-AS1* and *ADGB* in the TCGA data of tissues with endogenous *ADGB* expression (Fig. 4a). On the contrary, both genes showed a positive correlation in their expression in this dataset (R = 0.35). Since the *STXBP5-AS1* gene is located directly downstream of the *ADGB* gene on human chromosome 6, an open chromatin conformation could possibly affect both genes simultaneously. We also

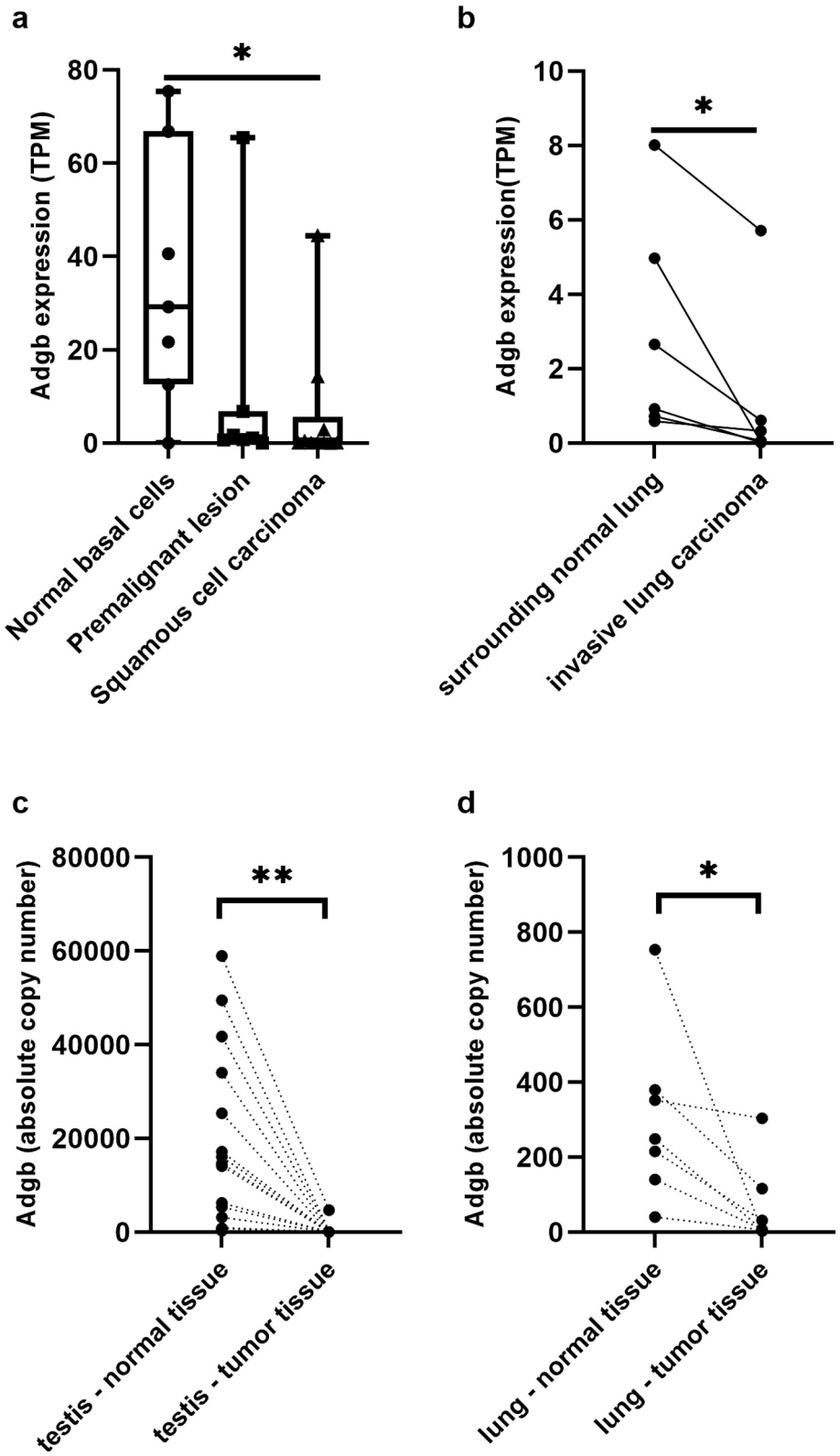

Fig. 1. Expression of *ADGB* mRNA in human tumor tissue. a) *ADGB* mRNA expression decreases significantly during progression from normal basal cells of the lung to squamous cell carcinoma (RNA-Seq data set from Ooi et al. 2014, PRJNA213155) b) *ADGB* mRNA expression is also significantly lower in invasive lung carcinoma (data set from Morton et al. 2014, PRJNA227275). Although there is high variability in the amount of *ADGB* mRNA in normal tissue samples, it decreases in every patient analyzed during tumor progression. c) + d) qPCR analysis of human *ADGB* mRNA levels in paired normal and tumor tissue samples of testis (n = 23) and lung (n = 7) cancer. *ADGB* mRNA expression is significantly lower in both types of tumor tissue biopsies. a) one-way ANOVA with multiple hypothesis correction; b) unpaired *t*-test; c)d) paired *t*-test; * = $p < 0.05$, ** = $p < 0.01$.

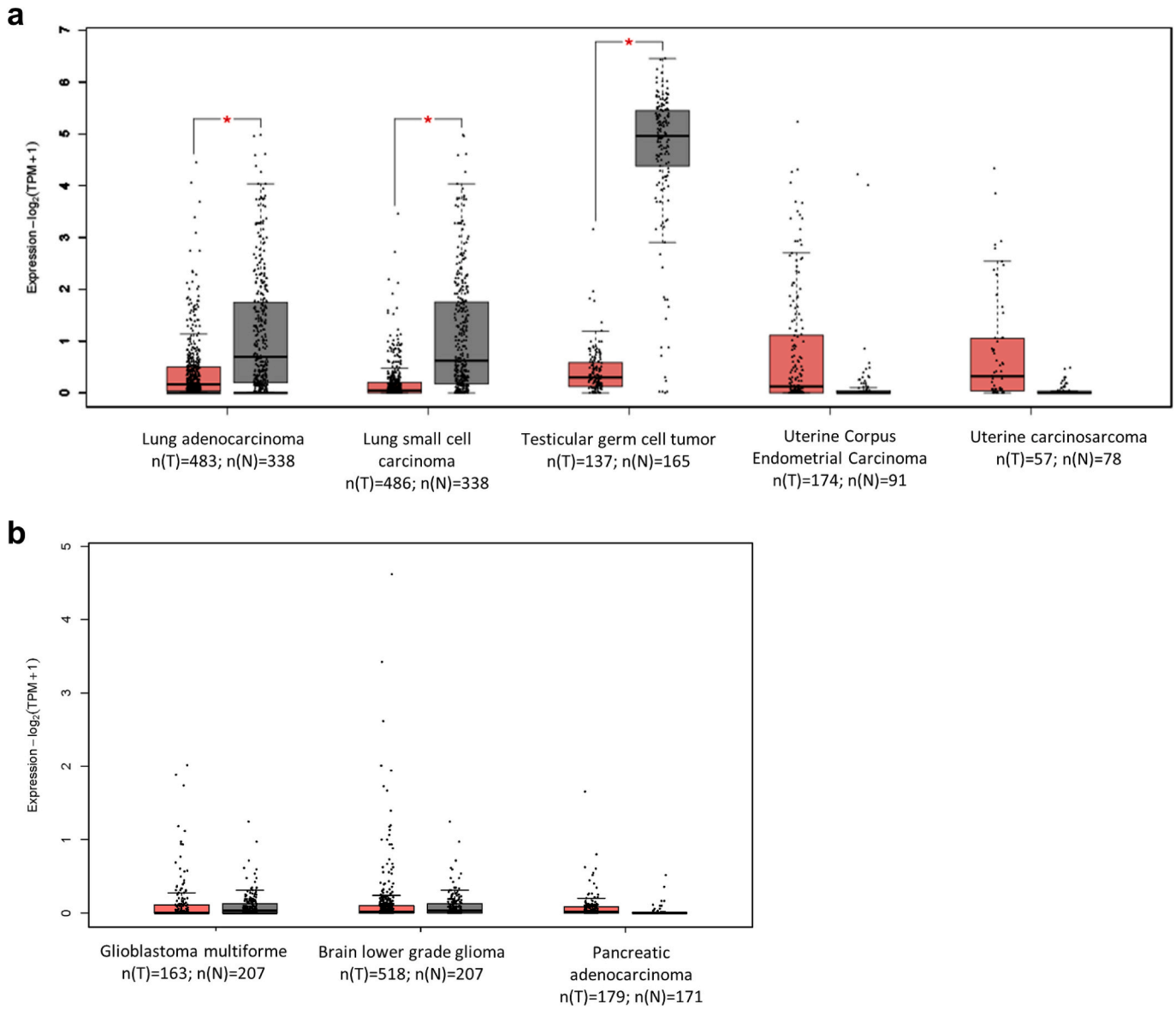

Fig. 2. *ADGB* expression in subsets of tumors sequenced by the TCGA consortium. Red = tumor tissue; grey = normal tissue. Numbers of tumor or healthy tissue entities that were used for the analysis are given under the corresponding graph. Expression is displayed as $\log_2$ of the TPM (transcripts per million) plus a pseudocount of 1. a) Expression of *ADGB* in tumors which resulted from tissues with endogenous *ADGB* expression. *ADGB* is significantly downregulated in lung adenocarcinoma, lung small cell carcinoma as well as testicular germ cell tumors. In contrast, *ADGB* mRNA expression is higher in tumorous uterine tissues, but compared to normal tissue this difference is not significant. b) *ADGB* expression in glioblastoma multiforme, brain lower grade glioma, and pancreatic adenocarcinoma compared to the corresponding healthy tissue. Also here, differences in expression are not statistically significant. Only low levels of *ADGB* mRNA can be detected in all these groups. Statistical analysis was performed as described [50]. Briefly, expression data are first $\log_2(\text{TPM} + 1)$ transformed and the $\log_2$FC is defined as median (Tumor) − median (Normal). One-way analysis of variance (ANOVA) was performed. An adjusted p-value < 0.05 and LFC > 0.5 was considered significant.

analyzed the correlation coefficient of *ADGB* and *STXBP5-AS1* in pancreatic tissue separately since this is the tissue for which the mechanism was initially proposed. Also in this sub-dataset, we found no evidence of a negatively correlated expression pattern (R = 0.05) (Fig. 4b).

In another study we recently showed that overexpression of transcription factors FOXJ1 and RFX2 induced the endogenous expression of *ADGB* in HEK293 cells (Koay et al., 2021). Indeed, we found a positive correlation between *ADGB* mRNA and expression of *FOXJ1* (R = 0.53) as well as *RFX2* (R = 0.5) in the TCGA data. Interestingly, *ADGB* mRNA expression can take place with virtually no expression of *FOXJ1* at all (Fig. 4c, red box). In contrast, there was no *RFX2*-negative sample that proved *ADGB* positive (Fig. 4d). RFX2 should mechanistically stabilize FOXJ1 binding to its DNA targets during motile ciliogenesis (Quigley and Kintner, 2017) and cell culture experiments showed that RFX2 alone is not sufficient to induce *ADGB* expression (Koay et al., 2021). Our findings suggest the existence of additional, FOXJ1-independent regulatory mechanisms for *ADGB* mRNA expression in tissue samples. We therefore included other transcription factors in our correlation analysis. *RFX1* and *RFX3*, which are also known to be involved in regulation of ciliary transcription, showed the same positive correlation with *ADGB* expression (R = 0.4, R = 0.44, respectively) as *FOXJ1* and *RFX2* (Fig. 4e, f). *ADGB* positivity always coincided with *RFX1* and *RFX3* expression, similar to *RFX2*, but isolated expression of any of the three factors did not consistently result in *ADGB* mRNA expression. Collectively, correlation analyses suggested that, apart from FOXJ1 and RFX2, also RFX3 could be functionally involved in *ADGB* expression.

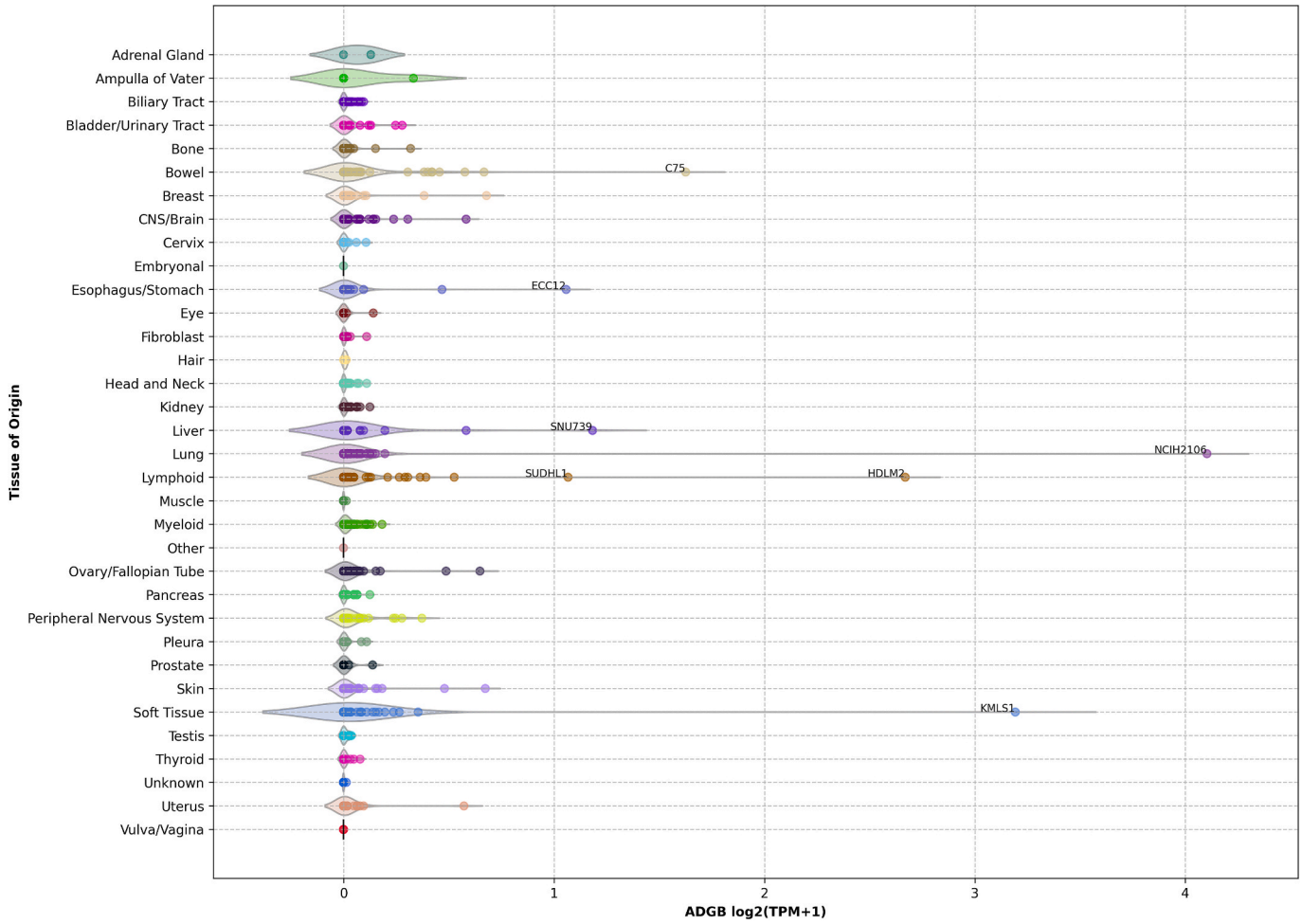

Fig. 3. *ADGB* mRNA expression in cancer cell lines analyzed by the CCLE and Human Protein Atlas consortia. Expression data was downloaded from the Human Protein Atlas web page. Only 3 cancer cell lines, NCIH2106, HDLM-2 and KMLS1 express endogenous levels of *ADGB* mRNA. Raw data are deposited under accession numbers PRJNA523380 and PRJNA10044209.

2.3. Transfection of RFX3 induces endogenous ADGB mRNA expression and interacts with the promoter

Since RFX3 might be functionally involved in *ADGB* expression, we transfected RFX3 in two different mammalian cell models. Overexpression of RFX3 indeed induced endogenous *ADGB* mRNA expression in both HEK293 and MCF7 cells (Fig. 5a) and enhanced activity of an *ADGB* promoter-enhancer-driven reporter gene in luciferase assays (Fig. 5b). Further evidence of this regulatory mechanism can be found in mice: disruption of *Rfx2* as well as *Rfx3*, but not *Rfx1*, significantly reduces *Adgb* mRNA expression in *ex vivo* differentiated ependymal cells, even though *Rfx2* mutants did not display any visible ciliary phenotype (Lemeille et al., 2020). ChIP sequencing data suggest that this regulation is direct, since all Rfx factors occupy the *Adgb* promoter region [(Lemeille et al., 2020); Fig. 5c]. RFX3 is therefore an intriguing candidate for further studies on the regulation of the *ADGB* gene locus.

2.4. Overexpression of ADGB induces morphological changes in A549 cells

As shown above, none of the analyzed cell lines seemed to be an adequate model of endogenous *ADGB* expression for studying its function: expression levels were either extremely low, expression did not cover the complete *ADGB* gene locus, cell lines putatively carried duplications of the *ADGB* gene locus (complicating genetic KO experiments), or cell lines were derived from tissues which themselves are no native expression sites of *ADGB* in healthy organisms.

To study effects of ectopic *ADGB* expression in a cancer cell line, we decided to stably overexpress *ADGB* in the widely used A549 lung adenocarcinoma cell line, since the lung represents one of the major native *ADGB* expression sites. Overall, 10 clonal cell lines were generated through G418 selection, 5 of which expressed human full length *ADGB* and another 5 that contained an empty vector backbone as control. We validated *ADGB* overexpression on the mRNA level via qPCR and on the protein level by immunofluorescent staining of fixed cell samples (S2 Fig). ADGB antibody signal showed an even cytoplasmic distribution. Although ADGB carries a candidate nuclear localization signal, there was no evidence of ADGB import into the nucleus (Fig. 6 a, b, S2 Fig). Intriguingly, ADGB-positive A549 cells showed abnormally long cellular appendages (Figs. 6c,d), also including cytokinetic bridges, with a median length of 10.52 μm vs. 4.49 μm in empty control cells. Rare outliers were even as long as 50 μm (Fig. 6d).

2.5. Transcriptomic changes in response to ADGB overexpression in A549 cells

To further characterize the molecular phenotype of ectopic *ADGB* expression, we performed RNA-seq analysis of stably transfected A549 cell clones (n = 3) in comparison to empty control cell lines (n = 3). TPM values for *ADGB* mRNA were 4.01, 1.90 and 0.57 and thus roughly comparable to the amount of *ADGB* mRNA in healthy lung samples (see also qPCR results in S2 Fig).

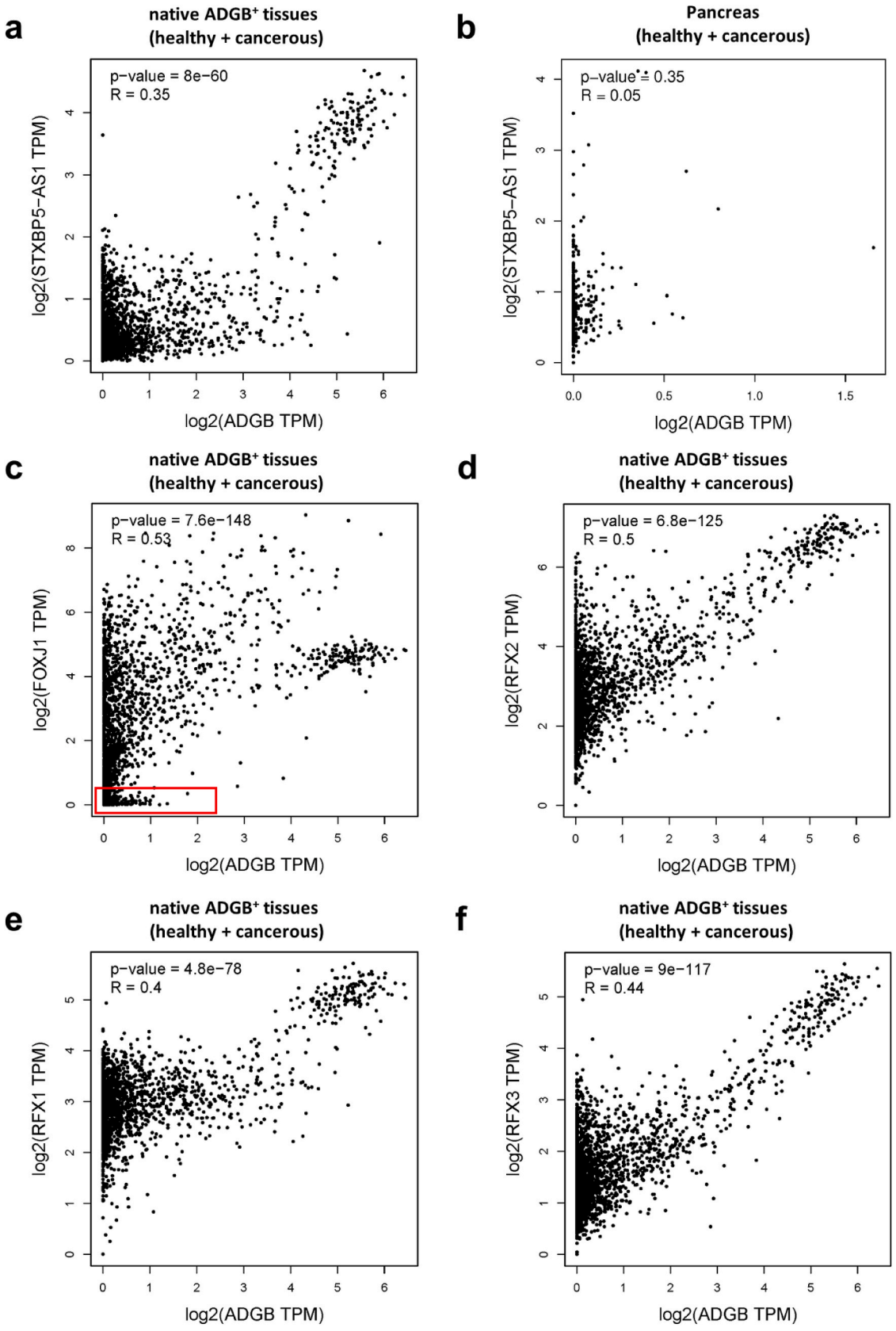

Fig. 4. Correlation analysis of *ADGB* and potential transcription factors on mRNA level. Data are from TCGA and GTEX, accessed from the GEPIA2 browser. *ADGB* expression is positively correlated with factors *STXBP5-AS1* [a)], *FOXJ1* [c)], *RFX2* [d)], *RFX1* [e)], and *RFX3* [f)] in RNA-Seq data derived from tissues with endogenous *ADGB* mRNA expression (testis, uterus, and lung) and matching tumor samples. In pancreatic cancer and healthy controls, *ADGB* mRNA is neither positively nor negatively correlated with the putative regulating anti-sense RNA *STXBP5-AS1* [b)].

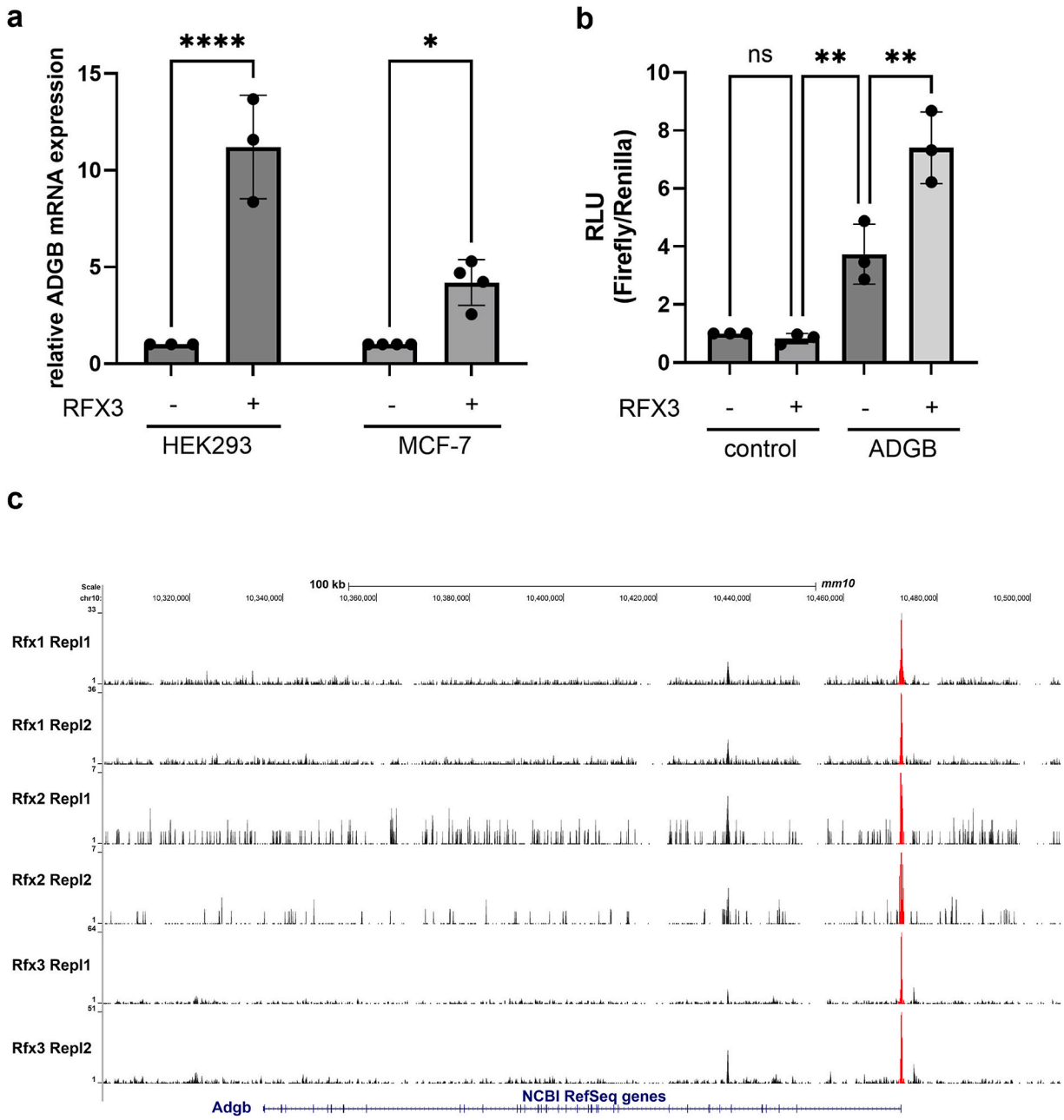

Fig. 5. Interaction of Rfx factors with the *ADGB* promoter. a) Overexpression of RFX3 induces endogenous expression of *ADGB* mRNA in HEK293 (n = 3) and MCF7 (n = 4) cells. b) Overexpression of RFX3 (n = 3) increases *ADGB* promoter/enhancer-driven luciferase activity c) Occupancy of Rfx transcription factors at the murine *Adgb* promoter. Transcription factors Rfx1, Rfx2 and Rfx3 show reproducible ChIP-Seq peaks in both replicates overlapping the promoter region upstream of the first exon (note that the murine *Adgb* locus is located on the opposite strand). Datasets from (Lemeille et al. 2020).

Differential gene expression analysis identified a set of 497 genes, 231 of which were upregulated in response to *ADGB* overexpression (S1 File). Among these differentially regulated genes, a distinct set was either fully induced (counts in vector-only-transfected cells = 0 in all three replicates) or downregulated (counts in ADGB-transfected cells = 0 in all three replicates) upon *ADGB* induction (Table 1). Noteworthy, many of the upregulated genes are natively expressed in tissues which are positive for endogenous *ADGB* mRNA expression. For example, expression of the lincRNA *EWSAT1* (Acc. AC027088.2) was strongly induced upon overexpression of *ADGB*. *EWSAT1* has been described as a potential oncogene in both colorectal cancer and osteosarcoma (Shen et al., 2021; Zhang et al., 2018b), but in healthy tissue it is predominantly expressed in testis. This gene and the others are potential candidates for further analyses of *ADGB*'s gene regulatory network.

We then performed GO overrepresentation analysis on the list of differentially expressed genes (S2 File). *ADGB* overexpression was strongly associated with transcriptional changes of genes associated with, among others, the extracellular matrix organization (GO:0030198), cell adhesion (GO:0016477) and cell migration (GO:0016477) (Fig. 7). A similar picture was obtained when only upregulated genes were used for GO analysis (S3 File). Comparison of our gene list against pathway databases resulted in hits for extracellular matrix organization [REACTOME,(Gillespie et al., 2022)] and epithelial-to-mesenchymal transition in both thyroid cells and colorectal cancer [WikiPathways,(Martens et al., 2021)].

To identify potential regulators involved in transcriptional changes induced by *ADGB* overexpression, we performed an upstream regulator analysis using the Ingenuity Pathway software suite (Qiagen). The

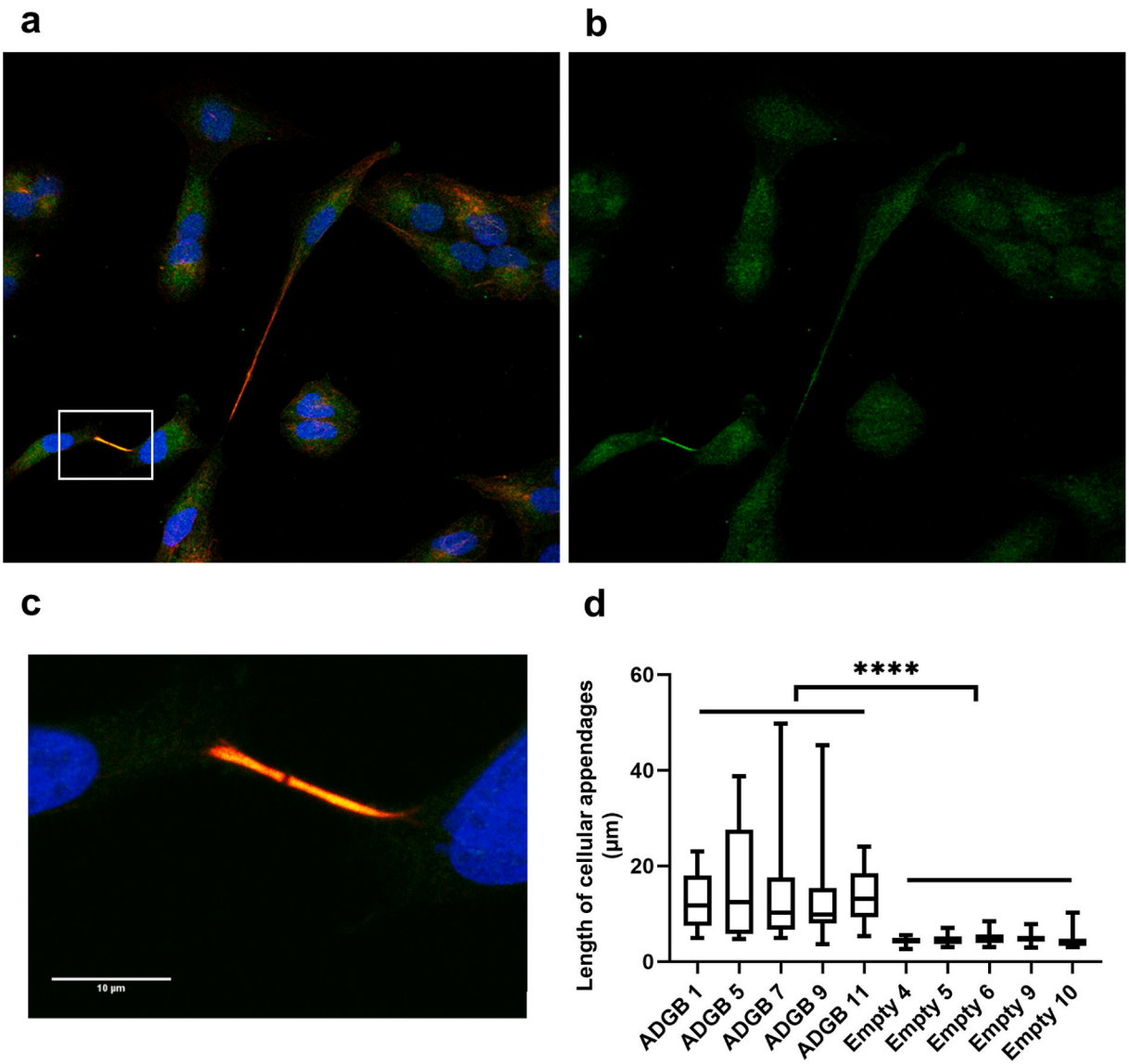

Fig. 6. Immunofluorescent staining of ADGB-overexpressing A549 cells. a) ADGB = green, DAPI (DNA) = blue; acetylated α-Tubulin = red; ADGB (isolated channel in b)) is localized in the cytoplasm and accumulates in cytokinetic bridges (enlarged in panel c)) which are also rich in tubulin. d) Ectopic expression of ADGB in A549 clones significantly increased the length of cellular appendages in comparison to cells transfected with an empty vector backbone as control. ADGB positive samples and empty samples from different clones were combined for statistical analysis. n(ADGB) = 79; n(Empty) = 84. Due to the large variability in appendage size, we performed a Wilcoxon rank sum test. **** p <= 0.0001.

resulting activated (blue) or deactivated (red) regulators are summarized in S1 Table. We evaluated the literature on these regulators regarding their influence on the motility of cells. Due to the proposed involvement of ADGB in cilia/flagella formation (Keppner et al., 2022; Koay et al., 2021) and its possible calcium, NO or oxygen reactivity (Hoogewijs et al., 2012; Nie et al., 2025; Reeder et al., 2024), we also investigated the upstream regulators with respect to these terms. Indeed, many of these candidate regulators turned out to be associated with ciliogenesis or were even known to influence motility or length of cilia. Few, however, were connected with oxygen or NO metabolism in literature. In line with the GO term analysis of the target genes, many of the predicted regulators were involved in modulating the motility of cells or in regulating the epithelial-to-mesenchymal transition.

3. Discussion

ADGB is a chimeric protein harboring a globin domain (Hoogewijs et al., 2012). Since other members of the globin protein family are known for differential regulation and potential oncogenic or protective functions in tumor entities, we studied the expression of *ADGB* in the context of cancer. Our data mining analysis of a wide variety of transcriptomes from cancer cell lines and different malignancies revealed that *ADGB* is not expressed in the majority of cell lines and downregulated in tumors derived from tissues with endogenous *ADGB* expression. This might suggest that *ADGB* either has a tumor suppressor function or simply no influence at all upon tumorigenesis. Counterintuitively, our transcriptome analysis of an *ADGB* overexpression system showed a putative oncogenic role for *ADGB*, in some agreement with two previous studies, which reported that downregulation of *ADGB* resulted in slower proliferation and higher rate of apoptosis of glioblastoma cells (Huang et al., 2014) and compromised stemness and metastatic capacity in pancreatic cancer cell lines (Chen et al., 2020). In our experiment, ectopic *ADGB* expression in A549 cells led to transcriptional changes which would promote cell motility and changes of the ECM, two processes relevant for the epithelial-to-mesenchymal transition and a hallmark of malignant cancer (Grelet et al., 2017;

Table 1
Differentially expressed genes upon overexpression of *ADGB* in A549 lung cancer cells. All genes were either fully induced or downregulated in all replicates. LFC = LogFoldChange; p-adjusted = BH corrected p-value. *ADGB* expression sites in bold.

Gene Name	LFC	p-adjusted	RNA-type	main mRNA expression site (HPA + GTEX)
AC027088.2	10.99	8.71E-16	linc-RNA	**testis**, **brain**
ADGB	**8.33**	**5.47E-07**	**protein-coding**	**fallopian tube, testis, lung, brain; ciliated cells**
NMU	8.17	1.81E-07	protein-coding	esophagus, skin; squamous epithelial cells
LINC00648	7.69	4.39E-06	linc-RNA	broadly expressed
NELL2	7.69	8.23E-05	protein-coding	**brains**; neurons, T-cells
LINC02081	7.69	4.59E-06	linc-RNA	**testis**, **lung**
CTNND2	7.58	2.79E-05	protein-coding	**brain**
MAGEA1	7.38	1.82E-05	protein-coding	**testis**; spermatogonia, spermatocytes
JPH1	6.90	2.23E-03	protein-coding	broadly expressed; highest in Cardiomyocytes
GIMAP2	6.74	5.51E-03	protein-coding	lymphoid tissue; B-cells
GLI3	6.25	6.37E-02	protein-coding	broadly expressed; fibroblasts
SLC27A6	6.24	1.19E-02	protein-coding	broadly expressed, adrenal gland, **brain**, **fallopian tube**, heart muscle
RARRES3	4.48	5.32E-02	protein-coding	broadly expressed
WNT6	−4.00	5.63E-04	protein-coding	broadly expressed; Sertoli cells
OPRL1	−4.62	5.61E-04	protein-coding	**testis**; early &late spermatids
MUC5B	−4.98	6.64E-07	protein-coding	salivary gland; intestinal epithelial cells
ADGRL3	−5.62	1.91E-04	protein-coding	**brain**
AL645608.7	−5.99	1.45E-04	linc-RNA	broadly expressed, artery
S100P	−6.00	3.13E-04	protein-coding	bone marrow, stomach, urinary bladder
SELENBP1	−6.51	2.69E-05	protein-coding	intestine, liver
SLITRK4	−6.54	3.15E-15	protein-coding	adrenal gland, **brain**, skeletal muscle
LUM	−6.85	1.36E-06	protein-coding	gallbladder, placenta; fibroblasts
TNNC1	−7.20	1.47E-07	protein-coding	muscle; striated muscle cell
CCNYL2	−7.26	4.24E-05	pseudogene	**testis**
MYOCD	−7.72	1.15E-06	protein-coding	broadly expressed; fibroblasts
HOXA9	−8.06	6.29E-10	protein-coding	broadly expressed, highest in kidney; proximal tubular cells
ASAH2	−9.65	3.51E-15	protein-coding	intestine; enterocytes
LINC00839	−9.85	7.83E-15	linc-RNA	broadly expressed, kidney, spleen

Thiery et al., 2009). *ADGB*-overexpressing cells showed longer cellular appendages including cytokinetic bridges. These bridges are the final connection of two daughter cells which have completed mitosis. Since the process of final abscission is carefully timed (Nähse et al., 2017), longer bridges suggest a higher motility of the connected cells or a change in adhesive properties, much in line with the transcriptomic and regulator analysis of our cell model. ADGB + tumor cells appear to have a selective advantage *in vitro*. On the other hand, and importantly, our extensive transcriptome analyses revealed that *ADGB* mRNA simply is not expressed in substantial amounts in human cancer entities. Thus, the effects we measured in our *in vitro* cell model may be in fact insubstantial for research on tumorigenesis *in vivo*. Several examples of genes conferring both tumor-suppressing and oncogenic functions exist. Their dualistic properties may be explained by alternative splicing (e.g.: Kahles et al., 2018; Sebestyén et al., 2016; Zhang et al., 2021), resulting in isoforms that have different roles. It is therefore possible that the apparently contradictory roles of ADGB in cancer cell lines and real-life tumors originate from alternative splice forms. The oncogenic properties would then be mediated by the full-length mRNA, which we have introduced in the overexpression study. However, endogenous expression of *ADGB* in tumor samples is very low, or even non-detectable. It is therefore more likely that the *ADGB* gene locus itself is differentially regulated.

A limitation of our study is its focus on the transcriptional expression levels. Nevertheless, our conclusions are supported by antibody stainings: no evidence of ADGB protein could be detected in cancerous lung, uterus and brain tissue, and only rare occurrences of signal were detected in renal and testis cancer (https://www.proteinatlas.org/ENSG00000118492-ADGB/pathology) (Uhlen et al., 2015). Future studies should focus on whether these observations are confirmed in expanded and independent cohorts.

In healthy tissues, *ADGB* is exclusively expressed in ciliated cells of lung, brain and the fallopian tubes as well as during late stages of spermatogenesis (Koay et al., 2021). The overexpression of FOXJ1 and RFX2, which are important ciliogenesis transcription factors, resulted in *ADGB* induction *in vitro* (Koay et al., 2021). We have found here that tissues can be positive for *ADGB* mRNA without expression of *FOXJ1*, possibly hinting at additional regulatory mechanisms for *ADGB* expression *in vivo*. We report evidence that the *ADGB* gene might be inducible by RFX3, and that other members of the RFX transcription factor family can bind to its promoter region. Thus, regulation of the *ADGB* gene is probably more complex than hitherto described (Herwig et al., 2024; Koay et al., 2021). The downregulation of *ADGB* in cells and cancerous tissues is probably not a result from epigenetic silencing: histone modification as well as DNase-hypersensitivity data from the ENCODE project suggest open chromatin at the *ADGB* promoter region [S3 Figure, (Koay et al., 2021)]. It is therefore possible that *ADGB* expression is actively silenced or requires synergistic activation via multiple transcription factors at once.

Ciliogenesis is a process which is tightly connected to the cell cycle: the centriole acts both as a initiation point for the spindle apparatus and as the basal body, which migrates to the cell borders and serves as an axoneme nucleation point to initiate cilium protrusion (Avasthi and Marshall, 2012). The cilium can then be absorbed upon re-entry into mitosis. In contrast to this, differentiation to a cell carrying motile cilia is rarely reversible. Notably, over-proliferative cells such as cancer cell lines and most malignancies *in vivo* do not carry motile cilia. This is probably due to the dedifferentiation in e.g. lung cancer types (Masciale et al., 2024; Pan et al., 2022). GO term enrichment analysis performed on differentially expressed genes between TCGA LUSC cancer samples and healthy controls resulted in enrichment of several ciliary terms, indicating dysregulation of ciliogenesis in these tumors (S4 Figure, Supplementary file S4). In our study, we find that this loss of the differentiation status of cells and tissues during cancer progression is accompanied by the loss of *ADGB* expression, indicating that ADGB is specifically needed in fully differentiated ciliated cells and also tightly regulated with this process.

In conclusion, ADGB may have the capability to enhance malignancy in tumor entities, and does so in artificial overexpressing cell systems, but since its expression is simply not induced *in vivo* in proliferative, cancerous tissues, ADGB probably does not exert a fundamental role in tumorigenesis.

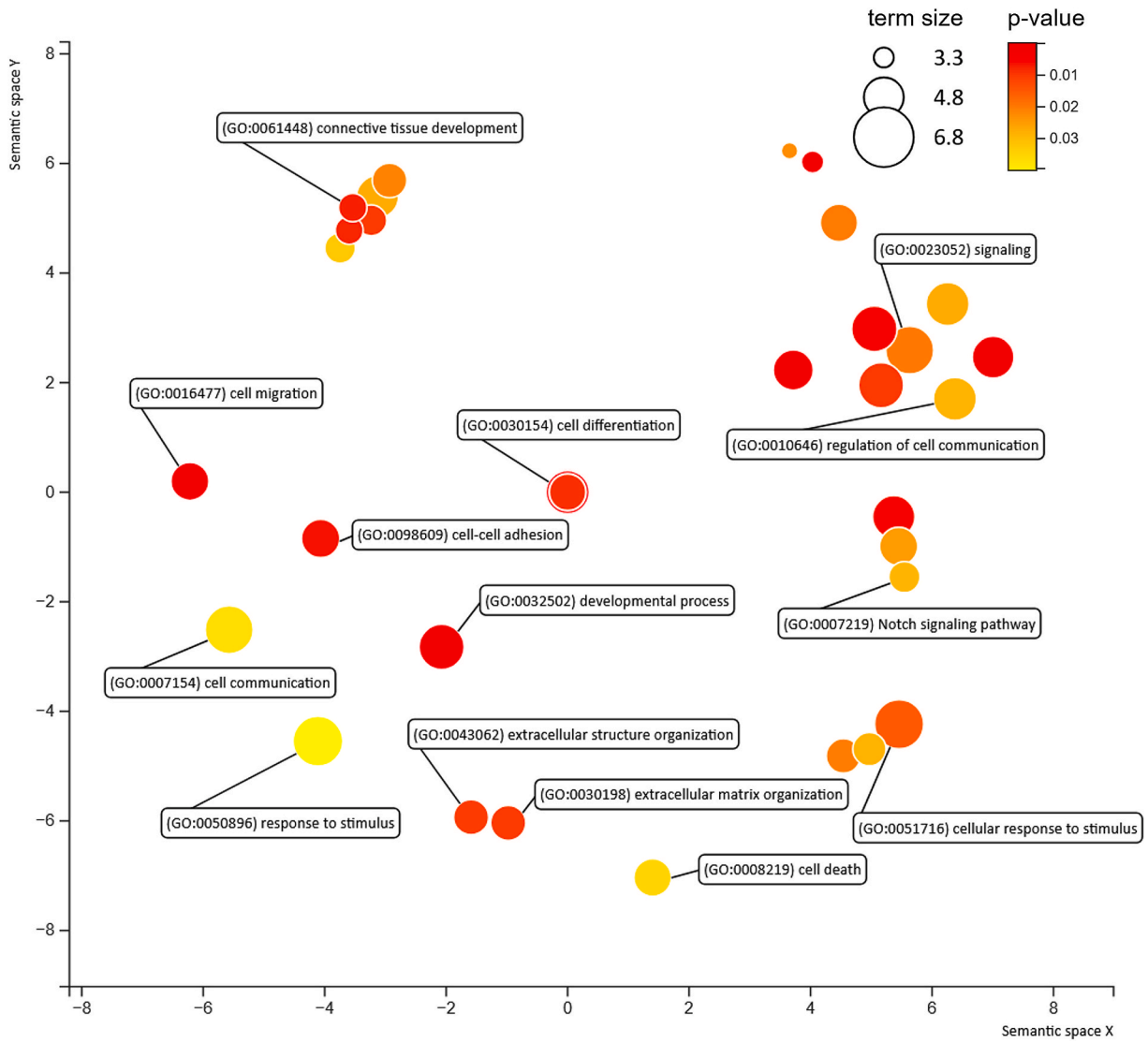

Fig. 7. GO terms enriched in gene lists derived from the comparison of ADGB+ vs. ADGB- transcriptomes. Terms were reduced and visualised with Revigo.

4. Methods

4.1. Ethical approval

Usage of human sample material from the tissue collection was approved by the ethics commission of the Landesärztekammer Rheinland-Pfalz (837.229.16/10548) on 12/07/2016. Due to the retrospective nature of the study, the ethics commission of the Landesärztekammer Rheinland-Pfalz waived the need of obtaining additional informed consent. All research was performed in accordance with guidelines and regulations of the Declaration of Helsinki.

4.2. RNA-sequencing (RNA-Seq) transcriptome analysis

RNA-seq libraries were prepared from 1000 ng of total RNA with Illuminás *TruSeq RNA Sample Prep Kit v2*, including poly-A selection, and sequenced as 70 nt single-end reads on an Illumina HiSeq2500. Library preparation and sequencing was performed by the NGS Core Facility of the Department of Biology, Johannes Gutenberg University (Mainz, Germany). Raw sequencing data are available at the European Nucleotide Archive under accession number PRJEB72248.

4.3. Processing of RNA-seq data

Raw transcriptome data were downloaded either from NCBI or ENA web servers (https://www.ncbi.nlm.nih.gov/sra; https://www.ebi.ac.uk/ena). Trimming parameters were assessed for each dataset via inspection with FastQC (https://www.bioinformatics.babraham.ac.uk/projects/fastqc/). Adapter and quality trimming were performed with BBDuk (https://sourceforge.net/projects/bbmap/). Minimum quality cutoff of all datasets was phred 20, minimal read length was 20 bp. After processing, the reads were mapped against the reference genome of *Homo sapiens* (Hsa 38) with HISAT2 under default parameters (Kim et al., 2019). Calculation of transcripts-per-million values (TPM) was performed with StringTie (Pertea et al., 2015) in guided mode.

4.4. Differential gene expression and GO term analysis

Differential gene expression analysis was conducted in R (https://www.r-project.org/) with Bioconductor package DESeq2 (Love et al., 2014). Genes were considered significant with BH p-adjusted ≤ 0.1. GO term enrichment analysis on gene lists with subsequent term reduction and visualization was performed with g:profiler (Raudvere et al., 2019) and Revigo (Supek et al., 2011).

4.5. Prediction of upstream regulators

Upstream regulators were predicted on lists of differentially expressed genes with a tool from the Core Ingenuity pathway analysis software (IPA, Qiagen). Chemical regulators were not in the biological focus of the present study and thus excluded from the analysis. Upstream regulators with a Z-Score > |2| and a BH-corrected p-value > 0.05 were considered significant. Further information regarding the calculation of these scores ca be found in the white paper (https://resources.qiagenbioinformatics.com/white-papers/Regulator_Effects_in_IPA.pdf).

4.6. Analysis of TCGA RNA-Seq datasets

RNA-seq data from the TGCA Cancer Genome Atlas Program (https://www.cancer.gov/ccg/research/genome-sequencing/tcga) were filtered by tumor type, analysed and visualized with the GEPIA 2 tool (Tang et al., 2019). Only tumor types derived from native *ADGB* mRNA expression sites (Keppner et al., 2022; Koay et al., 2021) were considered. One-way ANOVA parameters for differential testing of *ADGB* expression were |LFC|=0.5 and p-value cutoff = 0.01. For correlation analysis, the rank-based Spearman correlation coefficient and p-value were calculated with the cor.test function as implemented in the GEPIA2 tool. For the differential expression analysis of lung cancer vs. control samples, STAR count data were downloaded with the TCGAbiolinks package (Colaprico et al., 2016) and processed with DESeq2 (padj < 0.05, |LFC| = 2).

4.7. Cell culture, transfection and selection

MCF-7 and HEK293T cells were cultured and maintained in DMEM (Thermo Fisher) medium supplemented with 10 % fetal bovine serum (Chemie Brunschwig) and 100 µg/ml Pen/Strep Glutamine (Thermo Fisher), DMEM/FBS/PS for simplification, and incubated at 37 °C in a humidified incubator with 5 % CO_2. Cells were transfected using Roti-Fect (ROTH), according to manufacturer's instruction. Prior to transfection, cells were seeded on 24-well plates at a density of 5.2×10^4 cells per cm^2 of the dish surface area. For calcium phosphate precipitation method of DNA delivery, overnight medium was aspirated and replaced with DMEM/FBS/PS containing 25 µM chloroquine. In each well, 10 % (v/v) of transfection mixture was introduced to the cells, consisting of 50 % (v/v) 1.2 to 1.5 µg plasmid DNA/250 mM $CaCl_2$ and 50 % (v/v) HBS buffer (50 mM HEPES, 280 mM NaCl, 10 mM KCl, 1.5 mM Na_2HPO_4, 12 mM glucose). Transfected cells were incubated at 37 °C/5% CO_2 for 24 h before the medium was replaced with fresh DMEM/FBS/PS and continued to incubate at 37 °C/5% CO_2 for another 24 h. Cells were harvested 48 h post-transfection.

A549 cells were provided by Prof. Dr. Susanne Strand (University Medical Center, Mainz). Cells were cultured in DMEM supplemented with 10 % FBS and 1 % Pen/Strep (PAN Biotech) at room air with 5 % CO_2 and 37 °C. pcDNA3.1 vector with either full length human *ADGB* or an empty backbone as control were transfected using Lipofectamine 3000 (Invitrogen). Cells were selected with Geneticin (Roth) over 2 weeks and clones were obtained through single cell dilution. For each condition, several clones of independent integration events were used for further analysis.

4.8. Generation of expression plasmids

pLenti6.3/V5-DEST-RFX3 was purchased from DNASU (catalog no. HsCD00852582). pFLAG-CMV-RFX3 was cloned from there by the amplification of full-length *RFX3* with a primer pair (forward: 5′-AAAGCAGGAAGCTTGGTAGTGGTATGCAGACATCAGAGACTGG-3′, HindIII site underlined; and reverse: 5′-AGGCACAGGGTACCTTAGACTGCAGTGTAGGTATTTCCTG-3′, KpnI site underlined). The amplicon was digested and ligated to HindIII- and KpnI-linearized pFLAG-CMVTM-6a expression vector (Sigma-Aldrich) to generate pFLAG-CMV-RFX3. An overview over all primer sequences used in this study can be found in file S5.

4.9. RNA extraction

RNA extraction of tumor tissues was performed from snap-frozen samples with the RNeasy Plus Universal Mini kit (Qiagen) according to the manufacturer's instruction. ~ 50 mg of tissues was grinded and homogenized with a MiniLys (Precellys) system using mixed ceramic beads (Precellys Lysing CKMix, Precellys). RNA was eluted in nuclease-free water. RNA extraction from cell culture was performed with RNeasy Mini kit (Qiagen) according to the instructions of the manufacturer. RNA quality was assessed via a Bioanalyzer chip (Agilent), and only samples with RIN > 7 (for tissues) or > 9 (for cultured cells) were used for further analysis. RNA was quantified via Qubit measurement using the Broad Range RNA Assay Kit (Thermo Fisher) and stored at –80 °C until further use.

4.10. qRT-PCR

To validate RNA-Seq results, we performed quantitative reverse-transcription PCR (qRT-PCR) on tissues as described previously (Koay et al., 2021). 1000 ng of total RNA per sample was used for reverse transcription with the SuperScript III enzyme (10000 units per assay; Invitrogen) using an Oligo-dT primer. In the absence of validated reference genes, the amount of mRNA expression was normalized on the adjusted total amount of RNA. To additionally control for differences in cDNA synthesis, 100 ng of Drosophila total RNA was added to the reaction as a spike-in control. qRT-PCR was carried out using GoTaq qPCR Master Mix (Promega) on the ABI Prism 7500 Fast Detection System (SDS, Applied Biosystems, Carlsbad, USA) and interpreted using 7500 Software Version 2.3. Quantification of *ADGB* cDNA molecules (fwd primer: 5′-CGGAAGGAAAACATTCAAACAGG-3′; rev Primer: 5′-CGAAACTGATGAATTTCTTCCGC-3′) was done in absolute numbers applying a calibration standard curve with known amounts of target PCR product, previously cloned into the pGEM T-easy vector system (Promega). Copies of the Drosophila Globin 1 (Glob1) cDNA (fwd primer: 5′- GGAGCTAAGTGGAAATGCTCG-3′; rev primer: 5′-GATGATTCCGTAGACATGGTC-3′) of the internal control were measured in parallel to identify samples with substandard reverse transcription. For the RFX3-mediated induction, total RNA (2 µg) was reverse transcribed (RT) using the Prime Script RT reagent kit (Takara Bio USA) and cDNA levels were measured by qPCR (ADGB-Primer: Fwd-CCTGGAAACGTCCACAAGAT, Rev- GAGGAGGTTCCCCTGAAGTC) and a KAPA SYBR FAST qPCR reagent kit (Sigma-Aldrich) in a CFX96 C1000 Thermal Cycler (BioRad) with the following cycling parameters: Initial denaturation 5 min 95 °C; 40x (10 s 95 °C, 1:00 60 °C) including a melting curve ranging from 65 °C to 95 °C added at the end. Transcript levels were displayed as relative expression levels.

4.11. Luciferase reporter gene assays

Fifty nanograms of firefly luciferase plasmid containing the promoter-enhancer construct AP464-3AE (Koay et al., 2021) was co-transfected along with 1 ng of pRL-SV40 *Renilla* luciferase to control for differences in transfection efficiency and extract preparation as described previously (Randi et al., 2020). For RFX3 co-overexpression experiments, 300 ng of pFLAG-CMV-RFX3 was cotransfected with luciferase plasmid and the total amount of plasmid DNA used were normalized with pFLAG-CMV-6a empty vector. Luciferase activities were determined using the Dual Luciferase Reporter Assay System (Promega) and reported as relative firefly/*Renilla* luciferase activities. All reporter gene assays were performed at least three times independently.

4.12. Immunofluorescence

Cells were seeded in 24 well plates on uncoated glass cover slips. After 24–48 h, cells were fixed with 4 % PFA, washed, blocked in blocking buffer (1xPBS-TritonX with 5 % horse serum and 1 % BSA) and incubated with corresponding primary antibody [α-acetylated tubulin (T7451, Merck); custom made α-ADGB (Charles River Laboratories)] 1:500 in blocking buffer overnight. After several washing steps, cells were incubated with secondary antibody [CF 488, CF 555 or CF 633 conjugated anti-mouse/anti-rabbit F(ab)'-Fragment (Merck)] and counterstained with DAPI. Cover slips were mounted in RotiMount Fluorcare antifading solution (Roth) and sealed with Roti-Mount (Roth). Image acquisition was done with a Leica SP5. Cellular appendages were measured with ImageJ.

4.13. Statistical analysis

Statistical analysis was performed using Graph Pad Prism software (Version 8.4.3) for Windows.

CRediT authorship contribution statement

Carina Osterhof: Investigation, Visualization, Writing – review & editing, Validation, Writing – original draft, Conceptualization. **Michel Seiwert:** Investigation, Visualization. **Stefan Mündnich:** Investigation. **Teng Wei Koay:** Investigation, Writing – review & editing. **Elena Porto:** Investigation. **Glen Kristiansen:** Writing – review & editing, Resources. **David Hoogewijs:** Funding acquisition, Supervision, Visualization, Conceptualization, Project administration, Validation, Writing – review & editing. **Thomas Hankeln:** Conceptualization, Methodology, Resources, Writing – review & editing, Funding acquisition, Project administration, Supervision.

Funding

This work was supported by the Deutsche Forschungsgemeinschaft (DFG) to T.H. (HA 2103/9–1) and the Swiss National Science Foundation (SNSF) to D.H. (project grant 310030_207460).

Declaration of competing interest

The authors declare the following financial interests/personal relationships which may be considered as potential competing interests: Thomas Hankeln reports financial support was provided by German Research Foundation. David Hoogewijs reports financial support was provided by Swiss National Science Foundation. If there are other authors, they declare that they have no known competing financial interests or personal relationships that could have appeared to influence the work reported in this paper.

Acknowledgments

The results reported here are in part based upon data generated by the TCGA Research Network: https://www.cancer.gov/tcga. The authors thank Dr. Anne Bicker for help in analyzing qRT-PCR data and Dr. Gesa Poetzsch for critical reading of the manuscript.

Appendix A. Supplementary material

Supplementary data to this article can be found online at https://doi.org/10.1016/j.gene.2025.149840.

Data availability

Raw sequencing data haven been submitted to the European Nucleotide Archive under accession number ENA:PRJEB72248.

References

Avasthi, P., Marshall, W.F., 2012. Stages of ciliogenesis and regulation of ciliary length. Differ. Res. Biol. Divers. 83, S30. https://doi.org/10.1016/J.DIFF.2011.11.015.

Barretina, J., Caponigro, G., Stransky, N., Venkatesan, K., Margolin, A.A., Kim, S., Wilson, C.J., Lehár, J., Kryukov, G.V., Sonkin, D., Reddy, A., Liu, M., Murray, L., Berger, M.F., Monahan, J.E., Morais, P., Meltzer, J., Korejwa, A., Jané-Valbuena, J., Mapa, F.A., Thibault, J., Bric-Furlong, E., Raman, P., Shipway, A., Engels, I.H., Cheng, J., Yu, G.K., Yu, J., Aspesi, P., De Silva, M., Jagtap, K., Jones, M.D., Wang, L., Hatton, C., Palescandolo, E., Gupta, S., Mahan, S., Sougnez, C., Onofrio, R.C., Liefeld, T., MacConaill, L., Winckler, W., Reich, M., Li, N., Mesirov, J.P., Gabriel, S. B., Getz, G., Ardlie, K., Chan, V., Myer, V.E., Weber, B.L., Porter, J., Warmuth, M., Finan, P., Harris, J.L., Meyerson, M., Golub, T.R., Morrissey, M.P., Sellers, W.R., Schlegel, R., Garraway, L.A., 2012. The cancer cell line encyclopedia enables predictive modelling of anticancer drug sensitivity. Nature 483, 603–607. https://doi.org/10.1038/nature11003.

Burmester, T., Hankeln, T., 2014. Function and evolution of vertebrate globins. Acta Physiol. 211, 501–514. https://doi.org/10.1111/apha.12312.

Burmester, T., Weich, B., Reinhardt, S., Hankeln, T., 2000. A vertebrate globin expressed in the brain. Nature 407, 520–523. https://doi.org/10.1038/35035093.

Chen, S., Huang, L., Li, G., Qiu, F., Wang, Y., Yang, C., Pan, J., Wu, Z., Chen, J., Tian, Y., 2020. LncRNA STXBP5-AS1 suppresses stem cell-like properties of pancreatic cancer by epigenetically inhibiting neighboring androglobin gene expression. Clin. Epigenetics 12, 1–12. https://doi.org/10.1186/s13148-020-00961-y.

Colaprico, A., Silva, T.C., Olsen, C., Garofano, L., Cava, C., Garolini, D., Sabedot, T.S., Malta, T.M., Pagnotta, S.M., Castiglioni, I., Ceccarelli, M., Bontempi, G., Noushmehr, H., 2016. TCGAbiolinks: an R/bioconductor package for integrative analysis of TCGA data. Nucleic Acids Res. 44, e71.

De Backer, J., Maric, D., Zuhra, K., Bogaerts, A., Szabo, C., Vanden Berghe, W., Hoogewijs, D., 2022. Cytoglobin silencing promotes melanoma malignancy but sensitizes for ferroptosis and pyroptosis therapy response. Antioxid. Basel Switz. 11, 1548. https://doi.org/10.3390/antiox11081548.

Elsherbiny, M.E., Shaaban, M., El-Tohamy, R., Elkholi, I.E., Hammam, O.A., Magdy, M., Allalunis-Turner, J., Emara, M., 2021. Expression of myoglobin in normal and cancer brain tissues: correlation with hypoxia markers. Front. Oncol. 11, 1561. https://doi.org/10.3389/FONC.2021.590771/BIBTEX.

Fabrizius, A., Andre, D., Laufs, T., Bicker, A., Reuss, S., Porto, E., Burmester, T., Hankeln, T., 2016. Critical re-evaluation of neuroglobin expression reveals conserved patterns among mammals. Neuroscience 337, 339–354. https://doi.org/10.1016/j.neuroscience.2016.07.042.

Fiocchetti, M., Cipolletti, M., Ascenzi, P., Marino, M., 2018. Dissecting the 17β-estradiol pathways necessary for neuroglobin anti-apoptotic activity in breast cancer. J. Cell. Physiol. 233, 5087–5103. https://doi.org/10.1002/JCP.26378.

Flögel, U., Merx, M.W., Gödecke, A., Decking, U.K.M., Schrader, J., 2001. Myoglobin: a scavenger of bioactive NO. Proc. Natl. Acad. Sci. U. S. A. 98, 735–740. https://doi.org/10.1073/PNAS.98.2.735.

Flonta, S.E., Arena, S., Pisacane, A., Michieli, P., Bardelli, A., 2009. Expression and functional regulation of myoglobin in epithelial cancers. Am. J. Pathol. 175, 201–206. https://doi.org/10.2353/AJPATH.2009.081124.

Ghandi, M., Huang, F.W., Jané-Valbuena, J., Kryukov, G.V., Lo, C.C., McDonald, E.R., Barretina, J., Gelfand, E.T., Bielski, C.M., Li, H., Hu, K., Andreev-Drakhlin, A.Y., Kim, J., Hess, J.M., Haas, B.J., Aguet, F., Weir, B.A., Rothberg, M.V., Paolella, B.R., Lawrence, M.S., Akbani, R., Lu, Y., Tiv, H.L., Gokhale, P.C., de Weck, A., Mansour, A. A., Oh, C., Shih, J., Hadi, K., Rosen, Y., Bistline, J., Venkatesan, K., Reddy, A., Sonkin, D., Liu, M., Lehar, J., Korn, J.M., Porter, D.A., Jones, M.D., Golji, J., Caponigro, G., Taylor, J.E., Dunning, C.M., Creech, A.L., Warren, A.C., McFarland, J. M., Zamanighomi, M., Kauffmann, A., Stransky, N., Imielinski, M., Maruvka, Y.E., Cherniack, A.D., Tsherniak, A., Vazquez, F., Jaffe, J.D., Lane, A.A., Weinstock, D.M., Johannessen, C.M., Morrissey, M.P., Stegmeier, F., Schlegel, R., Hahn, W.C., Getz, G., Mills, G.B., Boehm, J.S., Golub, T.R., Garraway, L.A., Sellers, W.R., 2019. Next-generation characterization of the cancer cell line encyclopedia. Nature 569, 503–508. https://doi.org/10.1038/s41586-019-1186-3.

Gillespie, M., Jassal, B., Stephan, R., Milacic, M., Rothfels, K., Senff-Ribeiro, A., Griss, J., Sevilla, C., Matthews, L., Gong, C., Deng, C., Varusai, T., Ragueneau, E., Haider, Y., May, B., Shamovsky, V., Weiser, J., Brunson, T., Sanati, N., Beckman, L., Shao, X., Fabregat, A., Sidiropoulos, K., Murillo, J., Viteri, G., Cook, J., Shorser, S., Bader, G., Demir, E., Sander, C., Haw, R., Wu, G., Stein, L., Hermjakob, H., D'Eustachio, P., 2022. The reactome pathway knowledgebase 2022. Nucleic Acids Res. 50. https://doi.org/10.1093/NAR/GKAB1028. D687–D692.

Gorr, T.A., Wichmann, D., Pilarsky, C., Theurillat, J.P., Fabrizius, A., Laufs, T., Bauer, T., Koslowski, M., Horn, S., Burmester, T., Hankeln, T., Kristiansen, G., 2011. Old proteins – new locations: myoglobin, haemoglobin, neuroglobin and cytoglobin in solid tumours and cancer cells. Acta Physiol. 202, 563–581. https://doi.org/10.1111/J.1748-1716.2010.02205.X.

Grelet, S., McShane, A., Geslain, R., Howe, P.H., 2017. Pleiotropic roles of non-coding RNAs in TGF-β-mediated epithelial-mesenchymal transition and their functions in tumor progression. Cancers 9. https://doi.org/10.3390/CANCERS9070075.

Hendgen-Cotta, U.B., Merx, M.W., Shiva, S., Schmitz, J., Becher, S., Klare, J.P., Steinhoff, H.J., Goedecke, A., Schrader, J., Gladwin, M.T., Kelm, M., Rassaf, T., 2008. Nitrite reductase activity of myoglobin regulates respiration and cellular viability in myocardial ischemia-reperfusion injury. Proc. Natl. Acad. Sci. U. S. A. 105, 10256–10261. https://doi.org/10.1073/PNAS.0801336105/SUPPL_FILE/0801336105SI.PDF.

Herwig, A., Osterhof, C., Keppner, A., Maric, D., Koay, T.W., Mbemba-Nsungi, A., Hoogewijs, D., 2024. Ectopic MYBL2-mediated regulation of androglobin gene expression. Cells 13, 826. https://doi.org/10.3390/cells13100826.

Hoogewijs, D., Ebner, B., Germani, F., Hoffmann, F.G., Fabrizius, A., Moens, L., Burmester, T., Dewilde, S., Storz, J.F., Vinogradov, S.N., Hankeln, T., 2012. Androglobin: a chimeric globin in metazoans that is preferentially expressed in Mammalian testes. Mol. Biol. Evol. https://doi.org/10.1093/molbev/msr246.

Huang, B., Lu, Y., Li, X., Zhu, Z., Li, K., Liu, J., Zheng, J., Hu, Z., 2014. Androglobin knockdown inhibits growth of glioma cell lines. Int. J. Clin. Exp. Path. 7, 2179–2184.

Kahles, A., Lehmann, K.-V., Toussaint, N.C., Hüser, M., Stark, S.G., Sachsenberg, T., Stegle, O., Kohlbacher, O., Sander, C., Rätsch, G., 2018. Comprehensive analysis of alternative splicing across tumors from 8,705 patients. Cancer Cell 34, 211–224.e6. https://doi.org/10.1016/j.ccell.2018.07.001.

Keppner, A., Correia, M., Santambrogio, S., Koay, T.W., Maric, D., Osterhof, C., Winter, D.V., Clerc, A., Stumpe, M., Chalmel, F., Dewilde, S., Odermatt, A., Kressler, D., Hankeln, T., Wenger, R.H., Hoogewijs, D., 2022. Androglobin, a chimeric mammalian globin, is required for male fertility. eLife 11. https://doi.org/10.7554/eLife.72374.

Keppner, A., Maric, D., Correia, M., Koay, T.W., Orlando, I.M.C., Vinogradov, S.N., Hoogewijs, D., 2020. Lessons from the post-genomic era: Globin diversity beyond oxygen binding and transport. Redox Biol. 37, 101687. https://doi.org/10.1016/j.redox.2020.101687.

Kim, D., Paggi, J.M., Park, C., Bennett, C., Salzberg, S.L., 2019. Graph-based genome alignment and genotyping with HISAT2 and HISAT-genotype. Nat. Biotechnol. 37, 907–915. https://doi.org/10.1038/s41587-019-0201-4.

Koay, T.W., Osterhof, C., Orlando, I.M.C., Keppner, A., Andre, D., Yousefian, S., Alonso, M.S., Correia, M., Markworth, R., Schödel, J., Hankeln, T., Hoogewijs, D., 2021. Androglobin gene expression patterns and FOXJ1-dependent regulation indicate its functional association with ciliogenesis. J. Biol. Chem. 296. https://doi.org/10.1016/j.jbc.2021.100291.

Kono, H., Hosomura, N., Amemiya, H., Kawaida, H., Furuya, S., Akaike, H., Kawaguchi, Y., Sudo, M., Ichikawa, D., 2021. Cytoglobin as a prognostic factor for pancreatic ductal adenocarcinoma. Pancreas 50, 994–999. https://doi.org/10.1097/MPA.0000000000001871.

Kristiansen, G., Rose, M., Geisler, C., Fritzsche, F.R., Gerhardt, J., Lüke, C., Ladhoff, A.M., Knüchel, R., Dietel, M., Moch, H., Varga, Z., Theurillat, J.P., Gorr, T.A., Dahl, E., 2010. Endogenous myoglobin in human breast cancer is a hallmark of luminal cancer phenotype. Br. J. Cancer 102, 1736–1745. https://doi.org/10.1038/SJ.BJC.6605702.

Lemeille, S., Paschaki, M., Baas, D., Morlé, L., Duteyrat, J.-L., Ait-Lounis, A., Barras, E., Soulavie, F., Jerber, J., Thomas, J., Zhang, Y., Holtzman, M.J., Kistler, W.S., Reith, W., Durand, B., 2020. Interplay of RFX transcription factors 1, 2 and 3 in motile ciliogenesis. Nucleic Acids Res. 48, 9019–9036. https://doi.org/10.1093/nar/gkaa625.

Love, M.I., Anders, S., Huber, W., 2014. Differential analysis of count data - the DESeq2 package. Genome Biology. https://doi.org/10.1186/s13059-014-0550-8.

Martens, M., Ammar, A., Riutta, A., Waagmeester, A., Slenter, D.N., Hanspers, K., Miller, R.A., Digles, D., Lopes, E.N., Ehrhart, F., Dupuis, L.J., Winckers, L.A., Coort, S.L., Willighagen, E.L., Evelo, C.T., Pico, A.R., Kutmon, M., 2021. WikiPathways: connecting communities. Nucleic Acids Res. 49. https://doi.org/10.1093/NAR/GKAA1024. D613–D621.

Masciale, V., Banchelli, F., Grisendi, G., Samarelli, A.V., Raineri, G., Rossi, T., Zanoni, M., Cortesi, M., Bandini, S., Ulivi, P., Martinelli, G., Stella, F., Dominici, M., Aramini, B., 2024. The molecular features of lung cancer stem cells (LCSCs) in dedifferentiation process-driven epigenetic alterations. J. Biol. Chem. https://doi.org/10.1016/j.jbc.2024.107994.

Meller, S., van Ellen, A., Gevensleben, H., Bicker, A., Hankeln, T., Gorr, T.A., Sailer, V., Dröge, F., Schröck, F., Bootz, F., Schröck, A., Perner, S., Dietrich, D., Kristiansen, G., 2016. Ectopic myoglobin expression is associated with a favourable outcome in head and neck squamous cell carcinoma patients. Anticancer Res 36, 6235–6242. https://doi.org/10.21873/anticanres.11217.

Morton, M.L., Bai, X., Merry, C.R., Linden, P.A., Khalil, A.M., Leidner, R.S., Thompson, C. L., 2014. Identification of mRNAs and lincRNAs associated with lung cancer progression using next-generation RNA sequencing from laser micro-dissected archival FFPE tissue specimens. Lung Cancer 85, 31–39. https://doi.org/10.1016/j.lungcan.2014.03.020.

Nähse, V., Christ, L., Stenmark, H., Campsteijn, C., 2017. The abscission checkpoint: making it to the final cut. Trends Cell Biol. 27, 1–11. https://doi.org/10.1016/J.TCB.2016.10.001.

Nie, L.-S., Liu, X.-C., Han, H., Ren, Z.-H., Gao, S.-Q., Lin, Y.-W., 2025. Calmodulin interacts with androglobin and regulates the nitrite reductase activity. RSC Chem. Biol. 6, 175–181. https://doi.org/10.1039/D4CB00245H.

Oleksiewicz, U., Liloglou, T., Field, J.K., Xinarianos, G., 2011. Cytoglobin: biochemical, functional and clinical perspective of the newest member of the globin family. Cell. Mol. Life Sci. 2011 6823 68, 3869–3883. https://doi.org/10.1007/S00018-011-0764-9.

Ooi, A.T., Gower, A.C., Zhang, K.X., Vick, J.L., Hong, L., Nagao, B., Wallace, W.D., Elashoff, D.A., Walser, T.C., Dubinett, S.M., Pellegrini, M., Lenburg, M.E., Spira, A., Gomperts, B.N., 2014. Molecular profiling of premalignant lesions in lung squamous cell carcinomas identifies mechanisms involved in stepwise carcinogenesis. Cancer Prev. Res. (Phila. Pa.) 7, 487–495. https://doi.org/10.1158/1940-6207.CAPR-13-0372.

Pan, Z., Zhang, M., Zhang, F., Pan, H., Li, Y., Shao, Y., Yuan, X., Wang, J., Chen, J., 2022. Single-cell transcriptomics unveils the dedifferentiation mechanism of lung adenocarcinoma stem cells. Int. J. Mol. Sci. 24, 482. https://doi.org/10.3390/ijms24010482.

Pertea, M., Pertea, G.M., Antonescu, C.M., Chang, T.-C., Mendell, J.T., Salzberg, S.L., 2015. StringTie enables improved reconstruction of a transcriptome from RNA-seq reads. Nat. Biotechnol. 33. https://doi.org/10.1038/nbt.3122.

Quigley, I.K., Kintner, C., 2017. Rfx2 Stabilizes Foxj1 binding at chromatin loops to enable multiciliated cell gene expression. PLoS Genet. 13, 1–29. https://doi.org/10.1371/journal.pgen.1006538.

Randi, E.B., Vervaet, B., Tsachaki, M., Porto, E., Vermeylen, S., Lindenmeyer, M.T., Thuy, L.T.T., Cohen, C.D., Devuyst, O., Kistler, A.D., Szabo, C., Kawada, N., Hankeln, T., Odermatt, A., Dewilde, S., Wenger, R.H., Hoogewijs, D., 2020. The antioxidative role of cytoglobin in podocytes: implications for a role in chronic kidney disease. Antioxid. Redox Signal. https://doi.org/10.1089/ars.2019.7868.

Raudvere, U., Kolberg, L., Kuzmin, I., Arak, T., Adler, P., Peterson, H., Vilo, J., 2019. g: Profiler: a web server for functional enrichment analysis and conversions of gene lists (2019 update). Nucleic Acids Res. https://doi.org/10.1093/nar/gkz369.

Reeder, B.J., Deganutti, G., Ukeri, J., Atanasio, S., Svistunenko, D.A., Ronchetti, C., Mobarec, J.C., Welbourn, E., Asaju, J., Vos, M.H., Wilson, M.T., Reynolds, C.A., 2024. The circularly permuted globin domain of androglobin exhibits atypical heme stabilization and nitric oxide interaction. Chem. Sci. 15, 6738–6751. https://doi.org/10.1039/D4SC00953C.

Sebestyén, E., Singh, B., Miñana, B., Pagès, A., Mateo, F., Pujana, M.A., Valcárcel, J., Eyras, E., 2016. Large-scale analysis of genome and transcriptome alterations in multiple tumors unveils novel cancer-relevant splicing networks. Genome Res. 26, 732–744. https://doi.org/10.1101/gr.199935.115.

Shen, D., Liu, Y., Liu, Y., Wang, T., Yuan, L., Huang, X., Wang, Y., 2021. Long non-coding RNA EWSAT1 promoted metastasis and actin cytoskeleton changes via miR-24-3p sponging in osteosarcoma. J. Cell Mol. Med. 25, 716–728. https://doi.org/10.1111/JCMM.16121.

Supek, F., Bošnjak, M., Škunca, N., Šmuc, T., 2011. REVIGO summarizes and visualizes long lists of gene ontology terms. PLoS One 6, e21800. https://doi.org/10.1371/journal.pone.0021800.

Tang, Z., Kang, B., Li, C., Chen, T., Zhang, Z., 2019. GEPIA2: an enhanced web server for large-scale expression profiling and interactive analysis. Nucleic Acids Res. 47. https://doi.org/10.1093/NAR/GKZ430. W556–W560.

Thuy, L.T.T., Morita, T., Yoshida, K., Wakasa, K., Iizuka, M., Ogawa, T., Mori, M., Sekiya, Y., Momen, S., Motoyama, H., Ikeda, K., Yoshizato, K., Kawada, N., 2011. Promotion of liver and lung tumorigenesis in DEN-treated cytoglobin-deficient mice. Am. J. Pathol. 179, 1050–1060. https://doi.org/10.1016/J.AJPATH.2011.05.006.

Thiery, J.P., Acloque, H., Huang, R.Y.J., Nieto, M.A., 2009. Epithelial-mesenchymal transitions in development and disease. Cell 139, 871–890. https://doi.org/10.1016/J.CELL.2009.11.007.

Uhlen, M., Fagerberg, L., Hallstrom, B.M., Lindskog, C., Oksvold, P., Mardinoglu, A., Sivertsson, A., Kampf, C., Sjostedt, E., Asplund, A., Olsson, I., Edlund, K., Lundberg, E., Navani, S., Szigyarto, C.-A.-K., Odeberg, J., Djureinovic, D., Takanen, J.O., Hober, S., Alm, T., Edqvist, P.-H., Berling, H., Tegel, H., Mulder, J., Rockberg, J., Nilsson, P., Schwenk, J.M., Hamsten, M., von Feilitzen, K., Forsberg, M., Persson, L., Johansson, F., Zwahlen, M., von Heijne, G., Nielsen, J., Ponten, F., 2015. Tissue-based map of the human proteome. Science 347, 1260419. https://doi.org/10.1126/science.1260419.

Wittenberg, J.B., Wittenberg, B.A., 2003. Myoglobin function reassessed. J. Exp. Biol. 206, 2011–2020. https://doi.org/10.1242/JEB.00243.

Wu, F., He, J., Deng, Q., Chen, J., Peng, M., Xiao, J., Zeng, Y., Yi, L., Li, Z., Tian, R., Jiang, Z., 2023. Neuroglobin inhibits pancreatic cancer proliferation and metastasis by targeting the GNAI1/EGFR/AKT/ERK signaling axis. Biochem. Biophys. Res. Commun. 664, 108–116. https://doi.org/10.1016/j.bbrc.2023.04.080.

Xu, H.W., Huang, Y.J., Xie, Z.Y., Lin, L., Guo, Y.C., Zhuang, Z.R., Lin, X.P., Zhou, W., Li, M., Huang, H.H., Wei, X.L., Man, K., Zhang, G.J., 2013. The expression of cytoglobin as a prognostic factor in gliomas: a retrospective analysis of 88 patients. BMC Cancer 13, 247. https://doi.org/10.1186/1471-2407-13-247.

Yassin, M., Kissow, H., Vainer, B., Joseph, P.D., Hay-Schmidt, A., Olsen, J., Pedersen, A. E., 2018. Cytoglobin affects tumorigenesis and the expression of ulcerative colitis-associated genes under chemically induced colitis in mice. Sci. Rep. 2018 81 8, 1–16. https://doi.org/10.1038/s41598-018-24728-x.

Zhang, B., Chang, M., Wang, J., Liu, Y., 2017. Neuroglobin functions as a prognostic marker and promotes the tumor growth of glioma via suppressing apoptosis. Biomed. Pharmacother. Biomedecine Pharmacother. 88, 173–180. https://doi.org/10.1016/j.biopha.2017.01.029.

Zhang, B., Liu, Y., Li, Y., Zhe, X., Zhang, S., Zhang, L., 2018a. Neuroglobin promotes the proliferation and suppresses the apoptosis of glioma cells by activating the PI3K/AKT pathway. Mol. Med. Rep. 17, 2757–2763. https://doi.org/10.3892/MMR.2017.8132/HTML.

Zhang, J., Lan, S.J., Liu, Q.R., Liu, J.M., Chen, X.Q., 2013. Neuroglobin, a novel intracellular hexa-coordinated globin, functions as a tumor suppressor in hepatocellular carcinoma via Raf/MAPK/Erk. Mol. Pharmacol. 83, 1109–1119. https://doi.org/10.1124/MOL.112.083634.

Zhang, R., Li, J.B., Yan, X.F., Jin, K., Li, W.Y., Xu, J., Zhao, J., Bai, J.H., Chen, Y.Z., 2018b. Increased EWSAT1 expression promotes cell proliferation, invasion and epithelial-mesenchymal transition in colorectal cancer. Eur. Rev. Med. Pharmacol. Sci. 22, 6801–6808. https://doi.org/10.26355/EURREV_201810_16146.

Zhang, Y., Qian, J., Gu, C., Yang, Y., 2021. Alternative splicing and cancer: a systematic review. Signal Transduct. Target. Ther. 6, 1–14. https://doi.org/10.1038/s41392-021-00486-7.